Inorganic Chemistry

Article

pubs.acs.org/IC

Formation of a Covalent Bond between a Polyoxometalate and Silica Covered by SiH Moieties

Eva Grinenval, François Bayard, Jean-Marie Basset, and Frédéric Lefebvre*

CPE Lyon, CNRS, UMR C2P2, LCOMS, Bâtiment CPE Curien, Université Lyon 1, 43 Boulevard du 11 Novembre 1918, F-69616 Villeurbanne, France

ABSTRACT: Dehydroxylated silica was modified by grafting reaction of $SiHMe_2$ groups. The resulting material was fully characterized by various methods including infrared and one- and two-dimensional solid-state NMR. This material can further react with dehydrated polyoxometalates (POMs), leading to the formation of a covalent POM−silica bond. In the case of $H_4PVMo_{11}O_{40}$, hydrogen released during the grafting reaction reduces the POM. This leads to the formation of two surface species, which can be reoxidized in presence of oxygen. In the case of $H_3PW_{12}O_{40}$, no reduction is observed. In both cases, ^{29}Si solid-state NMR shows that the POM−silica bond is covalent, contrary to what was observed in homogeneous conditions.

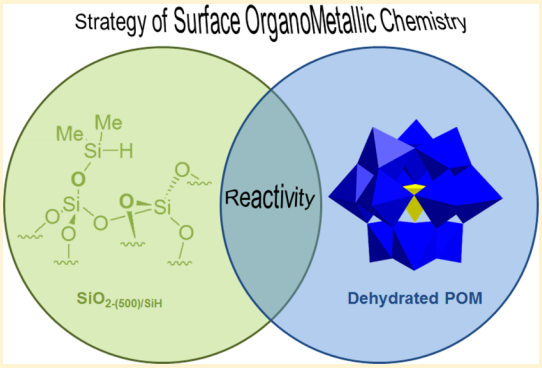

INTRODUCTION

Polyoxometalates (POMs) form a wide class of clusters formed by the assembly of transition metals from groups V and VI in their higher oxidation state (mainly M = Mo, W, V, Nb, Ta), highly π-donor oxo ligands O^{2-}, and heteroatoms (X). Heteroatoms can be transition metals or elements of the main groups.[1] The first and the most-known structure of such clusters is the one described by Keggin.[2] Keggin POMs show many advantages over other POMs, including stability and ease of synthesis. Their general formula is $[XM_{12}O_{40}]^{n-}$, with mainly X = P, Si, Ge, Co, Al and M = Mo, W. They are made of four groups $\{M_3O_{13}\}$ or triads surrounding the X heteroatom in a tetrahedral symmetry $\{XO_4\}$. Each triad is constituted by three octahedra $\{MO_6\}$, each of them being linked to the two others by sharing two edges of a same face.

POMs are therefore highly versatile and easily tunable to get the desired properties so that they find applications in various fields.[3−7] Among all these fields, catalysis is of prime interest due to the redox and acid/base properties of POMs.[8] The variety of possible POMs makes these compounds of great interest in chemical processes from research to industrial scales.[9,10] In particular the Keggin 11-molybdo-1-vanadophosphoric acid ($H_4PVMo_{11}O_{40}$) displays interesting catalytic activity for the oxidation of *i*-butane to methacrylic acid and methacrolein at rather high temperature (300−350 °C).[11] $H_4PVMo_{11}O_{40}$ is, in this case, (i) dehydrated, improving therefore the acid properties of this POM, and (ii) supported, improving therefore the accessibility to the active sites per surface unit. Except a recent article reporting the $H_4PVMo_{11}O_{40}$ immobilization onto mesoporous organically modified silica aerogels,[12] this catalyst is usually supported by conventional techniques (i.e., on silica or with large cations). This means that the active sites are not controlled, containing both highly dispersed and aggregated surface species.[13] Recent strategies were reported in the literature for the grafting of POMs on bare[14] or chlorinated[15] silica support, which open up new perspectives in POM-based materials. These strategies are based on the tools of surface organometallic chemistry (SOMC) and constitute an alternative method of covalent grafting compared to classical immobilization techniques of POMs that are sol−gel[16−20] and classical impregnation techniques. The principle consists in using (i) a partially dehydroxylated silica support bearing the desired functionality and (ii) the dehydrated POM corresponding to this functionality. Thus, it is possible to carefully control the distribution of POM units on silica support and to prevent the POM leaching. This late phenomenon takes place because POMs have a high solubility in polar solvents such as water or alcohols. Once dissolved, POMs interact electrostatically with cationic species. However, it is worth noting that once dehydrated, that is, after removal of the crystallization water molecules, cationic species and in particular acidic protons are not solvated anymore: these are isolated ("naked") resulting in, on one hand, an acidic strength increase and, on the other hand, a direct interaction between protons and POMs. This interaction was studied by different techniques including IR[21−24] and NMR[25,26] spectroscopies or density functional theory (DFT) calculations.[27−31] In this Article, we take advantage of this interaction to provide new POM-based materials. The reactivity of dehydrated tungsten- and molybdenum-based POMs with alkylsilane in homogeneous conditions was investigated in previous articles[32,33] and will constitute the basis for the synthesis and full characterization of

Received: September 12, 2013
Published: February 4, 2014

   dx.doi.org/10.1021/ic4023163 | *Inorg. Chem.* 2014, 53, 2022−2029

surface species reported in this Article. Thus, the strategy of SOMC is extending to a new kind of reactivity POM/support, providing therefore completely new well-defined surface species.

EXPERIMENTAL SECTION

General Procedure for the Preparation of Starting Materials. Heteropolyacids were synthesized from molybdenum oxide MoO_3 (99%, Acros), sodium molybdate Na_2MoO_4 (99+%, Aldrich), vanadium oxide V_2O_5 (99.6%, Acros), sodium metavanadate (>98%, Fluka), sodium phosphate $NaHPO_4$ (>99%, Aldrich), phosphoric acid H_3PO_4 (85%, Aldrich), and sulfuric acid H_2SO_4 (96%, Aldrich). Phosphotungstic acid $H_3PW_{12}O_{40}{\cdot}xH_2O$ (99.9+%, Aldrich) was used as received. Tetramethyldisilazane $(SiMe_2H)_2NH$ (97%, ABCR) was stored under argon and degassed prior to use. Oxygen was dried over 4 Å molecular sieves. Acetonitrile was purified according to published procedures, stored under argon, and degassed prior to use.[34]

All experiments were carried out by using standard air-free methodology in an argon-filled Vacuum Atmospheres glovebox, on a Schlenk line, or in a Schlenk-type apparatus interfaced to high vacuum line (10^{-5} Torr).

Gas-phase analyses were performed on a Hewlett-Packard 5890 series II gas chromatograph equipped with a flame ionization detector and a KCl/Al_2O_3 on fused silica column (50 m × 0.32 mm) or on an Intersmat IGC 120MB gas chromatograph equipped with a thermal conductivity detector and a molecular sieves column (5 Å; 2 m × 1/8″).

Elemental analyses were performed at the CNRS Central Analysis Department of Solaize or at the laboratory ICMUB of the University of Bourgogne at Dijon.

Diffuse reflectance Fourier-transformed infrared (DRIFT) spectra were recorded on a Nicolet 6700-FT spectrometer by using a cell equipped with CaF_2 or ZnSe windows, allowing in situ studies. Typically, 32 scans were accumulated for each spectrum (resolution 1 cm^{-1}).

The ^1H magic-angle spinning (MAS), ^{13}C cross-polarization (CP)-MAS, and ^{31}P MAS NMR spectra were recorded on a Bruker DSX-300 or a Bruker Avance 500 spectrometers equipped with a standard 4 mm double-bearing probehead. The ^{29}Si CP-MAS NMR spectra were recorded on a Bruker DSX-300 spectrometer equipped with standard 4 mm double-bearing probehead. Samples were introduced under argon in a zirconia rotor, which was then tightly closed. The spinning rate was typically 10 kHz. A typical cross-polarization sequence was used, with a 5 ms contact time and a recycle delay of 1−4 s to allow the complete relaxation of the ^1H nuclei. All chemical shifts are given with respect to tetramethylsilane (TMS) (for ^1H, ^{13}C and ^{29}Si) or 85 wt % H_3PO_4 (for ^{31}P), as an external reference.

Electron paramegnetic resonance (EPR) spectra were recorded using a Bruker Elexsys e500 X-band (9.4 GHz) spectrometer with a high sensitivity cavity at room temperature. The magnetic field was measured with a gaussmeter.

The calculations were done with $SiHMe_2$ groups grafted onto a (111) silica surface. A 100 ps molecular dynamic run was performed using the SYBYL software, which includes the force field developed by Clark et al.[35] The charge calculations were made with MMF94.[36] The sampling of interatomic distances was done every 0.1 ps during 70 ps after 30 ps of equilibration for the three Si−H hydrogen atoms.

Synthesis of 11-Molybdo-1-vanadophosphoric acid $H_4PVMo_{11}O_{40}{\cdot}xH_2O$. The 11-molybdo-1-vanadophosphoric acid was synthesized according to literature.[37] In a 250 mL round-bottomed flask, stoichiometric quantities of molybdenum oxide (19.17 g, 133.2 mmol) and vanadium oxide (1.10, 6.0 mmol) were introduced with 100 mL of water. Concentrated phosphoric acid (85%, 0.65 mL, 11.2 mmol) was added, and the reaction mixture was heated to reflux during 3 d under vigorous stirring. The solution was then filtered and precipitated by evaporation of water to give an orange solid. (Yield: 90%). ^{31}P NMR (D_2O) δ ppm: −3.96 (M); −3.79 (m). IR (KBr, cm^{-1}): 783 (s); 868 (m); 961 (s); 1062 (w); 1080 (sh). Elemental analyses: P 1.61 wt %, V 2.55 wt %, Mo 50.10 wt %. Molar ratios (theory): Mo/V 10.44 (11), P/V 1.04 (1).

Dehydration of Heteropolyacids. $H_3PW_{12}O_{40}$ was dehydrated by thermal treatment (2 h at 200 °C) under high vacuum (10^{-5} Torr). $H_4PVMo_{11}O_{40}$ was dehydrated by thermal treatment at 100 °C under high vacuum (10^{-5} Torr). These temperatures were chosen after performing a systematic study by ^1H MAS NMR as a function of the dehydroxylation temperature. The dehydrated heteropolyacids were stored under argon.

Preparation of $SiO_{2-(500)}$. The oxide support was Aerosil silica from Degussa. It was compacted with distilled water, dried at 140 °C for at least 5 d, sieved, calcined at 500 °C in air for 4−8 h, and partially dehydroxylated at 500 °C for 12 h under high vacuum (10^{-5} Torr). After this treatment the specific area was about 200 $m^2\ g^{-1}$, with an OH density of 1.4 OH nm^{-2} (0.465 mmol OH g^{-1}). IR (cm^{-1}): 3745 (s) ν(O−H). Solid-state MAS ^1H NMR (δ ppm): 1.8 (≡SiO**H**).

Modification of $SiO_{2-(500)}$ by $[(CH_3)_2SiH)_2NH]$. A mixture of tetramethyldisilazane $[(CH_3)_2SiH)_2NH]$ (1.6 mL, 5 equiv) in pentane (15 mL) and $SiO_{2-(500)}$ (3.9 g, 1.81 mmol of ≡SiOH) was stirred at 25 °C for 12 h. After filtration the solid was washed three times with pentane and dried for 15 min under vacuum at 25 °C and for 12 h at 150 °C under high vacuum (10^{-5} Torr). The resulting solid was white. Solid-state MAS ^1H NMR (δ ppm): 4.7 $[(\equiv SiO)Si\mathbf{H}(CH_3)_2]$; 0.0 $[(\equiv SiO)SiH(C\mathbf{H}_3)_2]$. CP-MAS ^{13}C NMR (δ ppm): −3 $[(\equiv SiOSiH(\mathbf{C}H_3)_2]$. CP-MAS ^{29}Si NMR (δ ppm): 0 $[(\equiv SiO)\mathbf{Si}H(CH_3)_2]$. IR ($cm^{-1}$): 2963 (m), 2907 (sh): ν(C−H). 2153 (s): ν(Si−H). 1423 (sh): δ(C−H). C 1.24 wt %.

Reactivity of Dehydrated Heteropolyacids with $SiO_{2-(500)/[SiH]}$. A mixture of dehydrated heteropolyacid (0.88 g (0.494 mmol) of $H_4PVMo_{11}O_{40}$ or 1.45 g (0.503 mmol) of $H_3PW_{12}O_{40}$) in acetonitrile (10 mL) and $SiO_{2-(500)/[SiH]}$ (1g, 0.52 mmol of SiH) was stirred at 25 °C for 12 h under argon. After removal of the solution, the resulting powder was washed three times with 10 mL of acetonitrile, dried for 1 h at room temperature under high vacuum (10^{-5} Torr), and stored under argon.

Reactivity of $H_4PVMo_{11}O_{40}/SiO_{2-(500)/[SiH]}$ with Dry Oxygen. The studied sample was loaded in a reactor of known volume under strict exclusion of air. After evacuation of argon, dry oxygen (typically around 100 Torr) was introduced. The system was heated for 12 or 15 h at 100 °C, and then the pressure of oxygen was measured by volumetry to know its consumption. The addition of dry oxygen was done twice.

RESULTS AND DISCUSSION

Partially Dehydroxylated and Silylated Silica Support. Functionalization of oxide surfaces is a widely known technique for catalyst preparation because it allows the tuning of the solid

dx.doi.org/10.1021/ic4023163 | Inorg. Chem. 2014, 53, 2022−2029

Scheme 1. Silylation of $SiO_{2-(500)}$ with TMDS

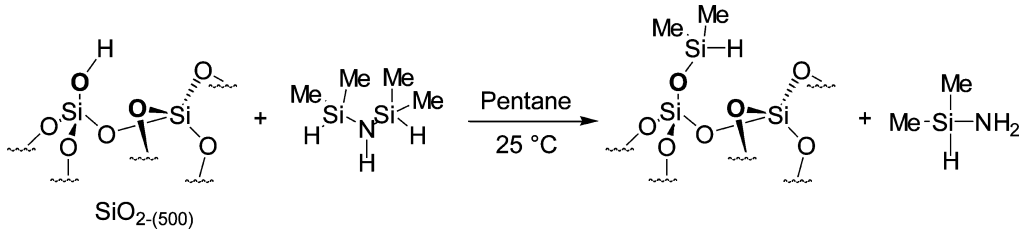

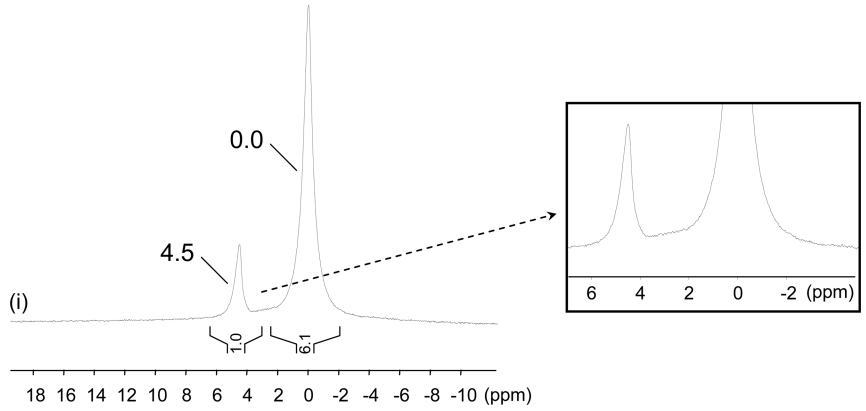

Figure 1. Solid-state ^{1}H MAS NMR spectra of $SiO_{2-(500)/[SiH]}$ recorded at 10 kHz.

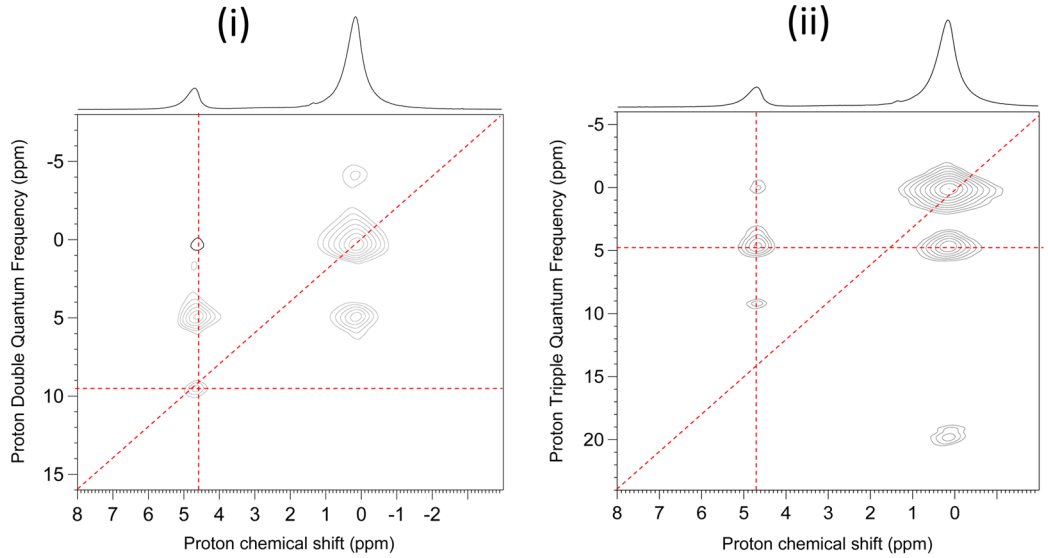

Figure 2. 2D ^{1}H MAS NMR spectra of $SiO_{2-(500)/[SiH]}$: (i) DQ; (ii) TQ.

adsorption properties and the control of the amount and nature of the reactive sites.[38] Silylating agents such as chlorosilanes, alkoxysilanes, and silazanes are commonly used in the case of silicon-based oxide supports. Among the various silylating reagents (chlorosilanes, alkoxysilanes, and silazanes), silylation of $SiO_{2-(500)}$ was performed with 1,1,4,4-tetramethyldisilazane (TMDS),[39] because it reacts at room temperature without the need of a catalyst and also because it only releases an amine that is easily removed under high vacuum at moderate temperature. This yields a functionalized silica support, which is written as $SiO_{2-(500)/[SiH]}$ in the following (Scheme 1).

With $SiO_{2-(500)}$, which contains 0.465 mmol OH g^{-1}, the reaction of TMDS yields quantitatively $SiO_{2-(500)/[SiH]}$ as evidenced by solid-state NMR and in situ IR spectroscopy. After the gas-phase reaction of $SiO_{2-(500)}$ with TMDS, followed by desorption of the sample under vacuum at 150 °C, the IR spectrum of the resulting solid showed the disappearance of the ν(O−H) band at 3745 cm^{-1} and the appearance of new bands at 2160 cm^{-1}, assigned to ν(Si−H), and at 2963, 2907, and 1423 cm^{-1}, corresponding, respectively, to ν(C−H) and δ(C−H) of Si−CH_3 groups. This is consistent with the selective and complete consumption of the silanols, which are transformed into SiH surface groups.

The ^{1}H MAS NMR spectrum of $SiO_{2-(500)/[SiH]}$ (Figure 1) shows only two resonances at 0.0 and 4.5 ppm of 6.0/1.0 relative intensities, corresponding to the Si**C**$\underline{\mathbf{H}_3}$ and Si$\underline{\mathbf{H}}$ functions of the $SiMe_2H$ surface groups, respectively. No signal was observed at 1.8 ppm, which confirms the complete

dx.doi.org/10.1021/ic4023163 | Inorg. Chem. 2014, 53, 2022−2029

consumption of the starting surface silanols. Note also the absence of signals of residual amine. The ^{13}C CP MAS NMR spectrum shows only a signal at −3 ppm ($SiCH_3$), while the ^{29}Si CP spectrum shows signals at −109 (≡Si−O−Si≡ bridges of the silica network near silane protons) and 0 ppm ($OSiMe_2H$). These data are also fully consistent with the selective and quantitative formation of $O-SiMe_2H$ surface groups in $SiO_{2-(500)/[SiH]}$.

The ^1H double quantum (DQ) MAS spectrum of $SiO_{2-(500)/[SiH]}$ was performed to determine whether silane functionalities grafted on silica were close to each other. The spectrum (Figure 2i) shows two autocorrelation peaks for the proton resonances at 0.0 and 4.7 ± 0.2 ppm (0.0 and 9.5 ppm in the ω_2 dimension). The autocorrelation peak corresponding to SiH groups shows unambiguously that two functionalities are in a close environment. Two correlation peaks for the proton resonance at 4.7 ppm in the ω_2 dimension were also observed, indicating that $SiCH_3$ and SiH of the $SiMe_2H$ surface groups are close to each other, as expected.

The ^1H triple quantum (TQ) MAS spectrum of $SiO_{2-(500)/[SiH]}$ (Figure 2ii) displays only one autocorrelation peak for the proton resonance at 0.0 ppm (0.0 ppm in the ω_2 dimension). No autocorrelation peak was observed for the SiH surface groups (no resonance observed at 14.1 ppm in the ω_2 dimension). This means that three silane functionalities are not in a close environment. As for the ^1H DQ spectrum, correlation peaks for the proton resonance at 4.7 ppm in the ω_2 dimension were observed, indicating that $SiCH_3$ and SiH of the $SiMe_2H$ surface groups are close to each other.

To understand these results, a molecular modeling study was performed. It was indeed previously reported that, on silica dehydroxylated at high temperature, many silanol groups are not distributed homogeneously on the surface but form nests of three Si−OH groups such as on the (1 1 1) cristobalite face (Scheme 2).[14]

Scheme 2. Nest of Three Silanol Groups on the Dehydroxylated Silica Surface

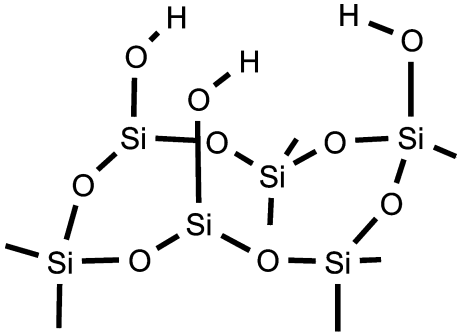

A dynamic study was then performed on the system depicted above and on the one bearing $SiHMe_2$ silane groups. For bare silica, the three protons can be located simultaneously at a distance lower than 5 Å from each other (see for example their disposition in Scheme 2), in agreement with the existence of a signal in the TQ ^1H spectrum. On the modified silica, the three protons of Si−H groups can never be located in such a disposition, only one distance being always lower than 5 Å (Figure 3).

According to elemental analysis, the C content in $SiO_{2-(500)/[SiH]}$ was 1.2 ± 0.1 wt %, which corresponds to a

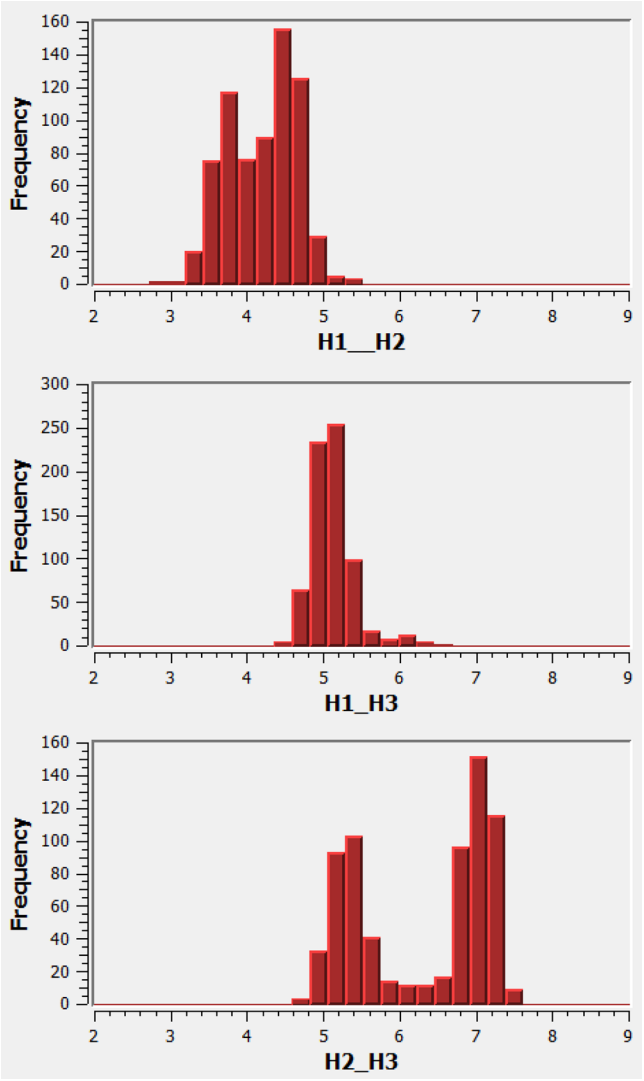

Figure 3. H−H distances between the three Si−H groups of a nest.

$SiMe_2H$ surface group density of 0.52 ± 0.05 mmol g^{-1}. This value is similar to the initial concentration of SiOH groups on $SiO_{2-(500)}$ (0.465 ± 0.005 mmol OH g^{-1}). The nitrogen content in the sample (<0.1 wt %, which corresponds to the detection limit) is in agreement with the complete absence of amine on the solid.

In conclusion, reaction of $SiO_{2-(500)}$ with TMDS yields selectively and quantitatively $SiO_{2-(500)/[SiH]}$, as evidenced by IR and solid-state NMR. Double and triple quantum NMR experiments and molecular modeling studies reveal that only two silane functionalities can be close to each other. The carbon content is similar to the expected amount, and no significant amount of residual amine or other surface species is detected on the surface.

Reactivity of Dehydrated $H_4PVMo_{11}O_{40}$ with $SiO_{2-(500)/[SiH]}$. When a $SiO_{2-(500)/[SiH]}$ pellet was immersed in a dimethyl sulfoxide (DMSO) solution containing an excess of dehydrated $H_4PVMo_{11}O_{40}$ (ca. 40 equiv per SiH), the solid took slowly a light green-blue color. After 12 h of reaction, the IR spectrum of the solid showed a new band in the 3230 cm^{-1} region related to the ν(OH) vibrational band of POM, while the IR band at 2155 cm^{-1}, characteristic of the initial SiH groups, was partially consumed (Figure 4). This result is

dx.doi.org/10.1021/ic4023163 | Inorg. Chem. 2014, 53, 2022−2029

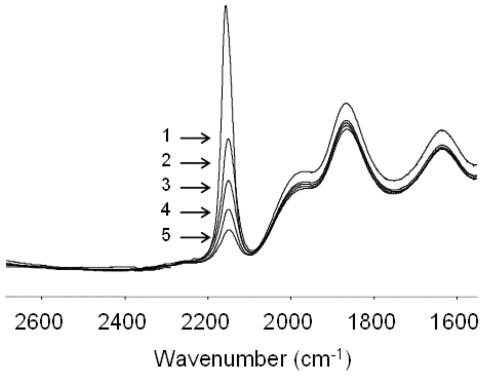

Spectrum	Description	ν(Si-H) (cm^{-1})	Area (a.u.)
1	$SiO_{2-(500)/[SiH]}$	2155	12.8
2	Dip #1	2148	6.9
3	Dip #2	2148	4.8
4	Dip #3	2147	1.2
5	Dip #4	2147	1.2

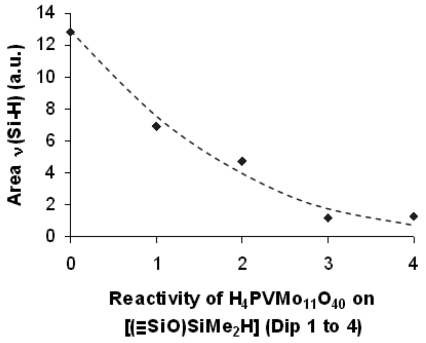

Figure 4. Reactivity of anhydrous $H_4PVMo_{11}O_{40}$ on $SiO_{2-(500)/[SiH]}$ (Dip 1−4): evolution of the ν(Si−H) vibrational band and integration of ν(Si−H) in the 2214−2097 cm^{-1} region.

Table 1. Addition of Dry Oxygen on $[H_4PVMo_{11}O_{40}/SiO_{2-(500)/[SiH]}]$ at 100 °C

addition of dry O_2	P_{O2} (mbar) introduced	measured	consumed	n_{O2} (mol) consumed	$O_2/H_4PVMo_{11}O_{40}$
1	69	61	9	9.9×10^{-6}	0.22
2	75	72	3	4.0×10^{-6}	0.09
total				1.4×10^{-5}	0.30

consistent with the reactivity of the Keggin-type POM 11-molybdo-1-vanadophosphoric acid with $SiO_{2-(500)/[SiH]}$, involving, therefore the cleavage of Si−H bonds and providing the solid referred to as $H_4PVMo_{11}O_{40}/SiO_{2-(500)/[SiH]}$ in the following. The pellet was then immersed again three times in the DMSO solution of dehydrated $H_4PVMo_{11}O_{40}$. The only difference observed on the IR spectra of the solid was the decrease of the ν(SiH) vibrational band (Figure 4).

To obtain analytical data, the reactivity of dehydrated $H_4PVMo_{11}O_{40}$ on $SiO_{2-(500)/[SiH]}$ was performed on a larger scale. For this purpose, a mixture of dehydrated $H_4PVMo_{11}O_{40}$ (0.88 g, 0.51 mmol) and $SiO_{2-(500)/[SiH]}$ (1.0 g, 0.52 mmol) was stirred in acetonitrile (10 mL) at room temperature for 12 h under argon. The solid turned gradually from orange to dark blue. After removal of the acetonitrile solution by filtration, the resulting powder was dried for 1 h at room temperature under high vacuum (10^{-5} Torr) and stored under argon. The resulting blue $H_4PVMo_{11}O_{40}/SiO_{2-(500)/[SiH]}$ sample contained 24.1 ± 0.2 wt % of Mo (1.1 POM/nm^2). This corresponds to 0.7 ± 0.1 POM per initial SiH silane surface group (while a POM/SiH ratio of 1.0 was used for the reaction). Moreover, similarly to the homogeneous reactivity,[33] no significant amount of hydrogen was observed in the gaseous phase during the grafting step.

Bulk dehydrated $H_4PVMo_{11}O_{40}$ is an orange compound, and supporting it on silica results in an orange solid. The solid obtained by mixing dehydrated $H_4PVMo_{11}O_{40}$ and $SiO_{2-(500)/[SiH]}$ at room temperature displays a clear color change. Consequently the introduction of SiH surface groups seems suitable with a modification of the POM units and furthers the POM/support interaction. The color change of the solid suggests indeed a reduction, at least partial, of the Keggin anions. Additions of dry oxygen were therefore carried out to measure its likely consumption. This was performed in a reactor of known volume (102 cm^3). Upon dry oxygen additions, the color change of $H_4PVMo_{11}O_{40}/SiO_{2-(500)/[SiH]}$ from dark blue to light yellow suggested clearly a reoxidation. The results, summed up in Table 1, show that 0.3 O_2 per $H_4PVMo_{11}O_{40}$ unit was consumed, corresponding to a mean of 1.2 electron reduction. This result, combined with the facts that hydrogen is soluble in organic solvents[40] and that the reactivity of this highly reducible POM with alkylsilanes is homogeneous,[33] explains the absence of hydrogen release.

The oxygen consumption of $H_4PVMo_{11}O_{40}/SiO_{2-(500)/[SiH]}$ reveals also unambiguously that the solid was initially reduced. The sample was therefore analyzed by solid-state ESR. The spectrum (Figure 5) is consistent with a signal of vanadyl species displaying the characteristic eight-line hyperfine pattern due to the interaction of unpaired electron with the ^{51}V nucleus (I = 7/2). This spectrum displays an axial symmetry with some dipolar interactions and is quite comparable to those observed when the concentration of spins is important.

Moreover, the $H_4PVMo_{11}O_{40}/SiO_{2-(500)/[SiH]}$ solid was compared to a standard sample of VO_2^+. This quantification enabled us to determine a spin number per Keggin unit of 0.6, corresponding to 0.6 $V^{(IV)}$/POM (instead of 1 $V^{(IV)}$/POM if all

dx.doi.org/10.1021/ic4023163 | Inorg. Chem. 2014, 53, 2022−2029

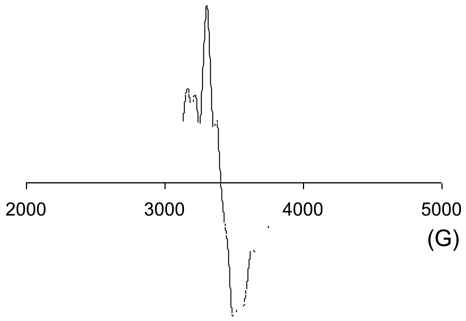

Figure 5. ESR spectrum of $H_4PVMo_{11}O_{40}/SiO_{2-(500)/[SiH]}$.

of the $V^{(V)}$ was reduced to $V^{(IV)}$. It is worth noting that this ESR quantification does not cover the whole oxygen consumption (1.2 electrons). This leads us to think that the sample contained probably a mixture of POM species with paired and unpaired electrons. In addition, it is possible that the sample contained unreduced POM.

To obtain further information about the characterization of $H_4PVMo_{11}O_{40}/SiO_{2-(500)/[SiH]}$, the solid-state $^{31}P\{1H\}$ NMR spectrum was recorded. This spectrum (Figure 6) displays two

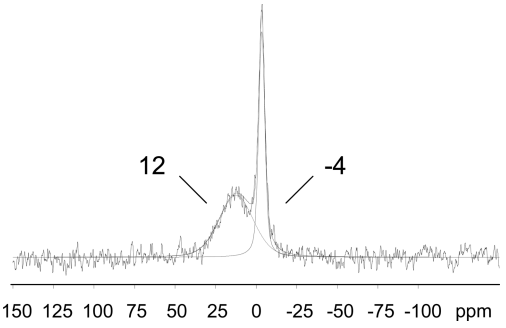

Figure 6. $^{31}P\{^1H\}$ MAS NMR spectrum of $H_4PVMo_{11}O_{40}/SiO_{2-(500)/[SiH]}$ recorded at 10 kHz.

resonances: a narrow one at −4 ppm and a broad and flattened one centered at 12 ppm with, respectively, 40/60 as relative intensities. The presence of these two signals confirms a mixture of species within the sample. −4 ppm is a rather usual chemical shift for a molybdic POM. However, +12 ppm is unusual. The differences of chemical shift and shape are clear and lead reasonably to the idea that there are different electronic environments for the POM phosphorus atom. The narrow signal at −4 ppm leads us to think of a species with paired electrons. As for the broad signal, both its shape and chemical shift lead us to think of a species with unpaired electrons. Apparently, the sample $H_4PVMo_{11}O_{40}/SiO_{2-(500)/[SiH]}$ is made of at least two POM species. Some similarities seem therefore to appear between oxygen addition, ESR, and NMR results.

To get even more understanding elements about the reoxidized sample, the ^{31}P MAS NMR spectrum of the corresponding solid, $H_4PVMo_{11}O_{40}/SiO_{2-(500)/[SiH]}@O_2$, obtained after addition of dry oxygen, was recorded. This spectrum (Figure 7) displays only one resonance at −2 ppm and can be reasonably ascribed to dehydrated $H_4PVMo_{11}O_{40}$. The presence of only one resonance shows clearly that the mixture obtained after reaction with the surface silane was reoxidized, leading to only one POM species.

The ^1H MAS NMR spectrum of $H_4PVMo_{11}O_{40}/SiO_{2-(500)/[SiH]}@O_2$ displays five resonances at 0.0, 1.8, 2.9, 4.7, and 7.8 ppm. The broad resonance at 7.8 ppm was assigned to the strong remaining acidity of the dehydrated POM. The signal at 4.7 ppm corresponds to unreacted Si−H groups, in agreement with IR data (Figure 4), while the one at 0 ppm corresponds to the protons of the $SiMe_2$ groups. It is not possible to differentiate methyl groups: $SiMe_2$ is in reacted and unreacted species. The two peaks at 1.8 and 2.9 ppm correspond to silanol groups (respectively, free and H-bonded silanols) formed during the POM oxidation by oxygen. The key result is the presence of strong acid sites on the POM, but no indication can be obtained from these data on the nature of the interaction linking POM and modified silica.

For this purpose, ^{29}Si CP-MAS NMR was carried out. ^{29}Si NMR spectroscopy is indeed used since a couple of decades ago for structure elucidation.[41−45] The spectrum of $H_4PVMo_{11}O_{40}/SiO_{2-(500)/[SiH]}@O_2$ (Figure 8) displays three

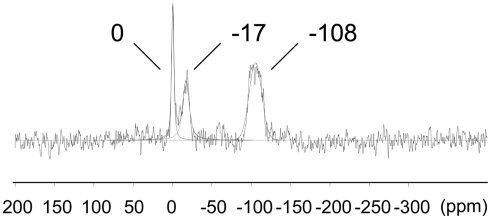

Figure 8. ^{29}Si solid-state CP-MAS NMR spectrum of $H_4PVMo_{11}O_{40}/SiO_{2-(500)/[SiH]}@O_2$.

resonances. Two of them, at 0 and −109 ppm, are observed on the starting modified silica and correspond, respectively, to

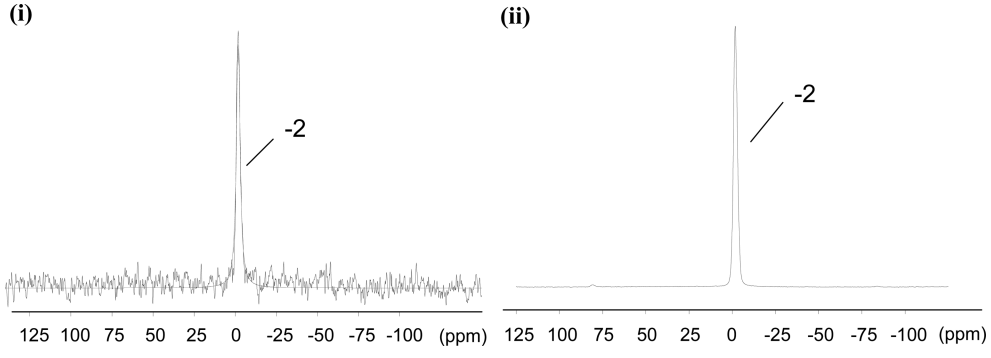

Figure 7. ^{31}P MAS NMR spectra. (i) $H_4PVMo_{11}O_{40}/SiO_{2-(500)/[SiH]}@O_2$ obtained after addition of dry oxygen. (ii) Bulk dehydrated $H_4PVMo_{11}O_{40}$ (2 h, 100 °C, 10^{-5} Torr).

dx.doi.org/10.1021/ic4023163 | Inorg. Chem. 2014, 53, 2022−2029

$OSiMe_2H$ and ≡Si−O−Si≡ bridges. The third one, at −17 ppm, can only be assigned to a silicon atom resulting from the reaction of the Si−H bond with the polyoxometalate. This chemical shift is consistent with the cleavage of the Si−H bond (note that a nonquantitative ^{29}Si CP sequence was used, preventing a comparison of the intensities of the various signals) and the insertion of an oxygen atom in its close environment because a $Si(R)_2(O_{1/2})_2$ (R = alkyl) unit displays a ^{29}Si signal at −21 ppm.[46] The formation of Si−Si bridges by a radical mechanism, which should lead to quite a similar chemical shift, is unlikely, due to the use of a dehydroxylated silica and to the distances between the Si−H groups.

All these results show clearly that a reaction occurs when the POM is contacted with the modified silica. It has been reported in the literature that $H_4PVMo_{11}O_{40}$ is not stable when it is reduced and decomposes, leading to free vanadium species and 12-molybdophosphate Keggin ions.[47−49] These two POMs have quite the same ^{31}P NMR chemical shift, preventing their differentiation by solid-state NMR, and thus, after reoxidation by oxygen, the presence of a mixture of these two POMs cannot be excluded, even if the conditions used here are quite different from what was previously observed in the literature. With this hypothesis, the ESR signal should arise from free vanadyl groups, and the other reduced species should be the 2-electron reduced 12-molybdophosphate. Another explanation should be that the two species observed by solid-state NMR are reduced molybdovanadophosphate, one with a vanadium(IV) and one with two Mo(V) ions. The above data cannot allow us to discriminate between these two possibilities.

Another point is that the ^{29}Si NMR chemical shift is very different from that observed when reacting directly the silane with the POM. Indeed in that case its value was ca. +60 ppm, and this result was explained by an ionic character of the bond between the POM and the silane moiety.[33] The value observed when the silane is grafted on silica corresponds to a covalent bond with the POM. The difference between the two cases is probably related to a different motion in the two cases. When the reaction is made in the homogeneous phase, there are only interactions between the POM and the silane, and the silane can jump from one oxygen to another, resulting in a pseudoionic character of the bond. In the case of a reaction with the surface, there are also interactions with the surface, resulting in a longer residence time at a given position. The result is then a chemical shift corresponding to a covalent bond. It should also be pointed out that it is not possible to determine, from these studies, if the POM is linked to the silica by one bond or more. Because of the close proximity of some $HSiMe_2$ groups, as shown by TQ ^1H MAS NMR, there is a priori no reason to exclude the formation of multigrafted species: the surface is probably covered (chemical analysis gives 1.1 POM per nm^2, corresponding to a monolayer) by mono- or digrafted POMs. This monolayer will also reduce the mobility, increasing the covalent character of the interaction between the support and the POM.

To further corroborate these data, the sample $H_3PW_{12}O_{40}/SiO_{2-(500)/[SiH]}$ was prepared from dehydrated $H_3PW_{12}O_{40}$ and $SiO_{2-(500)/[SiH]}$. In this case, no reduction phenomenon was observed, consistent with previous results in homogeneous conditions,[32] allowing the recording of the ^{29}Si CP-MAS NMR spectrum without addition of oxygen (Figure 9). Three resonances are observed at 0 ppm ($OSiMe_2H$), −108 ppm (Si−O−Si), and −18 ppm. Note that this third resonance is similar to the one observed for $H_4PVMo_{11}O_{40}/SiO_{2-(500)/[SiH]}@O_2$. This ^{29}Si chemical shift is different from those reported for a large variety of polytungstates containing covalent Si−O−W bonds: −44.6 ppm for $[(\gamma\text{-}PW_{10}O_{36})(t\text{-}BuSiOH)_2]^{3-}$,[50] −46.4 ppm for $[(PW_9O_{34})(t\text{-}BuSiOH)_3]^{3-}$,[51] and −65.6 ppm for $[(\gamma\text{-}SiW_{10}O_{36})(MeSiOH)_2]^{4-}$.[15] Surprisingly, this ^{29}Si chemical shift, ascribed to a silicon atom in interaction with the POM, was absolutely not in the same range of its homogeneous analogue $(Et_2MeSi)_3(PW_{12}O_{40})$. For this complex, a deshielding of silicon was indeed previously observed (56 and 60 ppm) and explained by a weak Si−O interaction with a more ionic character of the bond. Theoretical calculations confirmed that ^{29}Si NMR chemical shifts are greatly dependent on the Si−O distance conditions.[32] This suggests that for $H_3PW_{12}O_{40}/SiO_{2-(500)/[SiH]}$, a close interaction occurs between the POM and the oxide support, providing a probable ($O\underline{Si}Me_2-\underline{O}_{POM}$) species in which the POM is covalently linked to the oxide support. Note also the great analogy between the ^{29}Si NMR spectra of the two supported POMs.

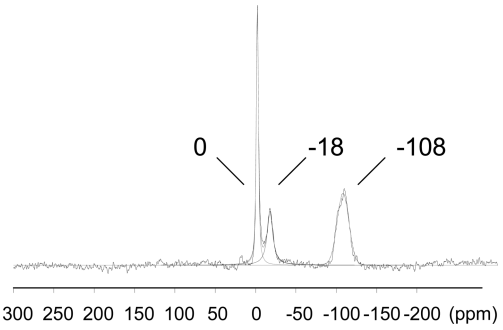

Figure 9. ^{29}Si solid-state CP-MAS NMR spectrum of $H_3PW_{12}O_{40}/SiO_{2-(500)/[SiH]}$.

CONCLUSION

In conclusion, upon the homogeneous reactivity of alkylsilane with dehydrated Mo- and W-based POMs described in previous articles, the SOMC strategy was applied to dehydrated 11-molybdo-1-vanadophosphoric acid on silica modified by silane surface groups. Full characterization results reported in this Article enabled the demonstration that this POM reacts with SiH surface groups, leading to a reduction phenomenon of both vanadium and molybdenum atoms, similar to homogeneous conditions. The main difference between homogeneous and heterogeneous systems is the kind of interaction linking the POM to the silica support. The use of silica modified by SiH surface groups led indeed to POMs covalently linked to the oxide support. Moreover, the use of partially dehydroxylated silica led to control of the POM loading. Therefore the SOMC approach applied to POMs is a way to get well-defined and well-distributed POM surface species. In addition the key added value of these new POM-based materials is the control of the POM-surface interaction.

AUTHOR INFORMATION

Corresponding Author

*E-mail: lefebvre@cpe.fr.

Notes

The authors declare no competing financial interest.

dx.doi.org/10.1021/ic4023163 | Inorg. Chem. 2014, 53, 2022−2029

REFERENCES

(1) Pope, M. T. *Heteropoly and Isopoly Oxometalates;* Springer-Verlag: Berlin, Germany1983.
(2) Keggin, J. F. *Proc. R. Soc. London* **1934**, *A144*, 75.
(3) Liu, R.; Li, S.; Yu, X.; Zhang, G.; Zhang, S.; Yao, J.; Keita, B.; Nadjo, L.; Zhi. *Small* **2012**, *8*, 1398−1406.
(4) Lv, H.; Geletii, Y. V.; Zhao, C.; Vickers, J. W.; Zhu, G.; Luo, Z.; Song, J.; Lian, T.; Musaev, D. G.; Hill, C. L. *Chem. Soc. Rev.* **2012**, *41*, 7572−7589.
(5) Seemann, K. M.; Bauer, A.; Kindervater, J.; Meyer, M.; Besson, C.; Luysberg, M.; Durkin, P.; Pyckhout-Hintzen, W.; Budisa, N.; Georgii, R.; Schneider, C. M.; Kögerler, P. *Nanoscale* **2013**, *5*, 2511.
(6) Thiel, J.; Molina, P. I.; Symes, M. D.; Cronin, L. *Cryst. Growth Des.* **2012**, *12*, 902−908.
(7) Wang, H.; Hamanaka, S.; Nishimoto, Y.; Irle, S.; Yokoyama, T.; Yoshikawa, H.; Awaga, K. *J. Am. Chem. Soc.* **2012**, *134*, 4918−4924.
(8) Song, Y.-F.; Tsunashima, R. *Chem. Soc. Rev.* **2012**, *41*, 7384−7402.
(9) Deng, W.; Zhang, Q.; Wang, Y. *Dalton Trans.* **2012**, *41*, 9817.
(10) Gaspar, A. R.; Evtuguin, D. V.; Neto, C. P. *Ind. Eng. Chem. Res.* **2004**, *43*, 7754−7761.
(11) Paul, S.; Courtois, V. L.; Vanhove, D. *Ind. Eng. Chem. Res.* **1997**, *36*, 3391−3399.
(12) Al-Oweini, R.; Aghyarian, S.; El-Rassy, H. *J. Sol-Gel Sci. Technol.* **2012**, *61*, 541−550.
(13) Grinenval, E.; Garron, A.; Lefebvre, F. *J. Catal.* **2013**, DOI: 10.1155/2013/828962.
(14) Grinenval, E.; Rozanska, X.; Baudouin, A.; Berrier, E.; Delbecq, F.; Sautet, P.; Basset, J. M.; Lefebvre, F. *J. Phys. Chem. C* **2010**, *114*, 19024−19034.
(15) Grinenval, E.; Basset, J.-M.; Lefebvre, F. *J. Inorg. Chem.* **2013**, DOI: 10.1155/2013/902192.
(16) Villanneau, R.; Marzouk, A.; Wang, Y.; Djamaa, A. B.; Laugel, G.; Proust, A.; Launay, F. *Inorg. Chem.* **2013**, *52*, 2958−2965.
(17) Zhang, R.; Yang, C. *J. Mater. Chem.* **2008**, *18*, 2691−2703.
(18) Schroden, R. C.; Blanford, C. F.; Melde, B. J.; Johnson, B. J. S.; Stein, A. *Chem. Mater.* **2001**, *13*, 1074−1081.
(19) Dufaud, V.; Lefebvre, F. *Materials* **2010**, *3*, 682−703.
(20) Lefebvre, F. Polyoxometalates Encapsulated in Inorganic Materials: Applications in Catalysis. In *New and Future Developments in Catalysis;* Suib, S. L., Ed.; Elsevier: San Francisco, CA, 2013; pp 265−288.
(21) Bielanski, A.; Datka, J.; Gil, B.; Malecka-Lubanska, A.; Micek-Ilnicka, A. *Catal. Lett.* **1999**, *57*, 61.
(22) Bielanski, A.; Malecka, A.; Kybelkova, L. *J. Chem. Soc., Faraday Trans. 1* **1989**, *85*, 2847.
(23) Lee, K. Y.; Mizuno, N.; Okuhara, T.; Misono, M. *Bull. Chem. Soc. Jpn.* **1989**, *62*, 1731.
(24) Rocchiccioli-Deltcheff, C.; Fournier, M. *J. Chem. Soc., Faraday Trans.* **1991**, *87*, 3913.
(25) Kozhevnikov, I. V.; Sinnema, A.; van Bekkum, H. *Catal. Lett.* **1995**, *34*, 213.
(26) Kozhevnikov, I. V.; Sinnema, A.; Jansen, R. J. J.; van Bekkum, H. *Catal. Lett.* **1994**, *27*, 187.
(27) Bardin, B. B.; Bordawekar, S. V.; Neurock, M.; Davis, R. J. *J. Phys. Chem. B* **1998**, *102*, 10817.
(28) Ganapathy, S.; Fournier, M.; Paul, J. F.; Delevoye, L.; Guelton, M.; Amoureux, J. P. *J. Am. Chem. Soc.* **2002**, *124*, 7821.
(29) Janik, M. J.; Davis, R. J.; Neurock, M. *J. Phys. Chem. B* **2004**, *108*, 12292.
(30) Janik, M. J.; Davis, R. J.; Neurock, M. *J. Am. Chem. Soc.* **2005**, *127*, 5238.
(31) Kolokolov, D. I.; Kazantsev, M. S.; Luzgin, M. V.; Jobic, H.; Stepanov, A. G. *ChemPhysChem* **2013**, *14*, 1783.
(32) Grinenval, E.; Basset, J. M.; Lefebvre, F. *Inorg. Chem.* **2010**, *49*, 8749−8755.
(33) Grinenval, E.; Basset, J. M.; Lefebvre, F. *Inorg. Chim. Acta* **2011**, *370*, 297−303.
(34) Perrin, D. D.; Armarego, W. L. F. *Purification of Laboratory Chemicals,* 3rd Ed.; Pergamon Press: Oxford, UK, 1988.
(35) Clark, M.; Cramer, R. D.; Opdenbosch, N. V. *J. Comput. Chem.* **1989**, *10*, 982−1012.
(36) Halgren, T. *J. Am. Chem. Soc.* **1990**, *112*, 4710−4723.
(37) Poeppl, A.; Manikandan, P.; Koehler, K.; Maas, P.; Strauch, P.; Boettcher, R.; Goldfarb, D. *J. Am. Chem. Soc.* **2001**, *123*, 4577.
(38) Oldroyd, R. D.; Sankar, G.; Thomas, J. M.; Ozkaya, D. *J. Phys. Chem. B* **1998**, *102*, 1849−1855.
(39) Anwander, R.; Nagl, I.; Widenmeyer, M.; Engelhardt, G.; Groeger, O.; Palm, C.; Roeser, T. *J. Phys. Chem. B* **2000**, *104*, 3532−3544.
(40) Brunner, E. *J. Chem. Eng. Data* **1985**, *30*, 269−273.
(41) Casanovasa, J.; Illasb, F.; Pacchioni, G. *Chem. Phys. Lett.* **2000**, *326*, 523−529.
(42) Grimmer, A.-R.; Peter, R.; Fechner, E.; Molgedey, G. *Chem. Phys. Lett.* **1981**, *77*, 331−335.
(43) Mägi, M.; Lippmaa, E.; Samoson, A.; Engelhardt, G.; Grimmer, A. R. *J. Phys. Chem. B* **1984**, *88*, 1518−1522.
(44) Moravetski, V.; Hill, J.-R.; Eichler, U.; Cheetham, A. K.; Sauer, J. *J. Am. Chem. Soc.* **1996**, *118*, 13015−13020.
(45) Ramdas, S.; Klinowski, J. *Nature* **1984**, *308*, 521−523.
(46) Harris, R. K.; Kennedy, J. D.; McFarlane, W. *NMR and the Periodic Table;* Academic Press: London, 1978.
(47) Brückner, A.; Scholz, G.; Heidemann, D.; Schneider, M.; Herein, D.; Bentrupa, U.; Kant, M. *J. Catal.* **2007**, *245*, 369.
(48) Ressler, T.; Timpe, O.; Girgsdies, F.; Wienold, J.; Neisius, T. *J. Catal.* **2005**, *231*, 279−291.
(49) Shinachi, S.; Yahiro, H.; Yamaguchi, K.; Mizuno, N. *Chem.—Eur. J.* **2004**, *10*, 6489.
(50) Mazeaud, A.; Dromzee, Y.; Thouvenot, R. *Inorg. Chem.* **2000**, *39*, 4735−4740.
(51) Joo, N.; Renaudineau, S.; Delapierre, G.; Bidan, G.; Chamoreau, L.-M.; Thouvenot, R.; Gouzerh, P.; Proust, A. *Chem.—Eur. J.* **2010**, *16*, 5043−5051.